Eur. Phys. J. Plus (2017) **132**: 434
DOI 10.1140/epjp/i2017-11686-2

THE EUROPEAN PHYSICAL JOURNAL PLUS

Regular Article

Nonlocal microstructure-dependent dynamic stability of refined porous FG nanoplates in hygro-thermal environments

Mohammad Reza Barati[a]

Aerospace Engineering Department & Center of Excellence in Computational Aerospace, Amirkabir University of Technology, Tehran, Iran

Received: 27 March 2017 / Revised: 14 June 2017
Published online: 20 October 2017 –

Abstract. Based on the generalized nonlocal strain gradient theory (NSGT), dynamic modeling and analysis of nanoporous inhomogeneous nanoplates is presented. Therefore, it is possible to capture both stiffness-softening and stiffness-hardening effects for a more accurate dynamic analysis of nanoplates. The nanoplate is in hygro-thermal environments and is subjected to an in-plane harmonic load. Porosities are incorporated to the model based on a modified rule of mixture. Modeling of the porous nanoplate is conducted according to a refined four-variable plate theory with fewer field variables than in the first-order plate theory. The governing equations and related classical and nonclassical boundary conditions are derived based on Hamilton's principle. These equations are solved for hinged nanoplates via Galerkin's method. It is shown that porosities, moisture rise, temperature rise, nonlocal parameter, strain gradient parameter, material gradation, elastic foundation and uniform dynamic load have a remarkable influence on the dynamic behavior of nanoscale plates.

1 Introduction

Excessive stresses due to drastic moisture and temperature gradients make engineering structures susceptible to failure. The influence of temperature is known as thermal effect and the influence of moisture absorption from the atmosphere is known as hygro-scopic effect. Since functionally graded (FG) structures are usually exposed to environmental conditions, analysis of the combined effect of moisture and temperature on their mechanical behavior is of great importance in the research community [1–4]. It is reported that increase in moisture percentage and temperature reduces the performance of FG structures and natural frequencies [5]. Also, exerting a sever temperature field may lead to thermal buckling of FG structures [6–8].

Functionally graded nanoplates can be synthesized and constructed in different ways, as reported in several papers [9–12]. They are building blocks of nano-electro-mechanical systems (NEMs) used as nanosensors and nanoactuators [13–15]. Investigation of the mechanical behavior of scale-free plates has been extensively conducted in the literature based on classical theories. However, these theories are unable to describe the size effects on the nanostructures. This problem is resolved using the nonlocal elasticity theory of Eringen [16,17], in which small-size effects are considered by introducing an additional scale parameter. According to the nonlocal stress field theory, the stress state at a given point depends on the strain states at all points. The nonlocal elasticity theory has been broadly applied to examine the static and dynamic behaviors of nanoscale structures [18–35].

However, analysis and modeling of FG nanoplates are performed by various researchers. The finite element vibration analysis of FG nanosize plates based on classical plate theory (CPT) was conducted by Natarajan *et al.* [36]. Based on the third-order plate theory, Daneshmehr and Rajabpoor [37] examined the buckling behavior of nonlocal graded nanoplates under different boundary conditions. Analysis of resonance frequencies of FG micro and nanoplates according to nonlocal elasticity and strain gradient theory was performed by Nami and Janghorban [38]. They used nonlocal and strain gradient theories separately and concluded that these theories have different mechanisms in the analysis of nanoplates. Application of the three-dimensional nonlocal elasticity theory in the static and vibration analysis of an FG nanoplate was investigated by Ansari *et al.* [39] based on the classical plate model. Based on the

[a] e-mail: mrb.barati@ymail.com

generalized differential quadrature method (GDQM), Daneshmehr and Rajabpoor [40] analyzed the vibrational behavior of higher-order FG nanoplates using the nonlocal stress field theory. Application of the four-variable plate theory in the vibration analysis of FG nanoplates was examined by Belkorissat *et al.* [41]. They stated that the presented plate model has fewer field variables compared to first-order and third-order plate theories. Based on the four-variable plate theory, the shear deformation effect is captured, while the governing equations are very similar to the classical plate theory. Barati [42] proposed a refined beam model for the forced vibration analysis of FG nanobeams with porosities. Wave propagation, buckling and vibration analyses of smart FG nanoplates under various physical fields are carried out by Ebrahimi and Barati [43–45] using different plate theories. A comprehensive investigation of bending, buckling and vibrational behaviors of FG nanoplates on an elastic medium was conducted by Sobhy [46]. Also, Khorshidi and Fallah [47] performed the buckling analysis of FG nanoplates via a general nonlocal exponential shear deformation plate model. Sobhy and Radwan [48] presented a new quasi 3D nonlocal plate theory for vibration and buckling of FGM nanoplates.

It is noticeable that all of the aforementioned studies on FG nanoplates have reported a stiffness-softening mechanism due to the nonlocality. Although Eringen's nonlocal elasticity theory (NET) is a suitable theory for the modeling of nanostructures, it has some shortcomings due to neglecting the stiffness-hardening mechanism reported in experimental works and strain gradient elasticity [49]. By using the nonlocal strain gradient theory (NSGT), Lim *et al.* [50] matched the dispersion curves of nanobeams with those of the experimental data. They concluded that NSGT is more accurate for modeling and analysis of nanostructures by considering both stiffness reduction and enhancement effects. Application of NSGT in the wave dispersion analysis of FG nanobeams was examined by Li *et al.* [51]. Also, some investigations were performed using NSGT on vibration and buckling of nanorods, nanotubes and nanobeams [52–56]. Also, Farajpour *et al.* [57] presented the buckling analysis of nanoplates via a nonlocal strain gradient plate model employing exact and differential quadrature methods. In another work, Farajpour *et al.* [58] presented the nonlocal strain gradient modeling of nano-mechanical vibrating piezoelectric mass sensors. Also, Ebrahimi *et al.* [59] applied NSGT for wave propagation analysis of FG nanoplates under thermal loading. Therefore, it is of great importance to analyze the vibration behavior of FG nanoplates via NSGT for the first time. Nanoplates are usually subjected to hygro-thermal environments during their construction or operational life [60,61]. Despite their importance, there is no study on the dynamic stability of FG nanoplates under hygro-thermal effects considering porosities.

This paper makes the first attempt to model a compositionally graded nanoporous nanoplate according to NSGT. The proposed modeling of nanoplates incorporates a nonlocal stress field parameter as well as a length scale parameter related to the strain gradient. Thus, stiffness enhancement or reduction observed in nanostructures are considered. The porosity-dependent material properties of the nanoplate are described via a new power-law function. Nonclassical boundary conditions related to NSG theory as well as governing equations are obtained using Hamilton's principle. By solving the governing equations, using Galerkin's method, natural frequencies of the nanoplate are obtained. The results show that the vibrational behavior of the nanoplate is significantly influenced by nonlocality, strain gradient parameter, hygro-thermal loading, material composition, elastic medium and geometrical parameters. The obtained frequencies can be used as benchmark results in the analysis of nanoplates modeled by nonlocal and microstructure-dependent strain gradient theories.

2 Nonlocal strain gradient nanoplate model

The proposed nonlocal strain gradient theory [50] takes into account both nonlocal stress field and the strain gradient effects by introducing two scale parameters. This theory defines the stress field as

$$\sigma_{ij} = \sigma_{ij}^{(0)} - \nabla\sigma_{ij}^{(1)}, \tag{1}$$

in which the stresses $\sigma_{ij}^{(0)}$ and $\sigma_{ij}^{(1)}$ correspond to strain ε_{ij} and strain gradient $\nabla\varepsilon_{ij}$, respectively, as

$$\sigma_{ij}^{(0)} = \int_V C_{ijkl}\alpha_0(x,x',e_0a)\varepsilon'_{kl}(x')\mathrm{d}x', \tag{2a}$$

$$\sigma_{ij}^{(1)} = l^2\int_V C_{ijkl}\alpha_1(x,x',e_1a)\nabla\varepsilon'_{kl}(x')\mathrm{d}x', \tag{2b}$$

in which C_{ijkl} are the elastic coefficients and e_0a and e_1a capture the nonlocal effects and l captures the strain gradient effects. When the nonlocal functions $\alpha_0(x,x',e_0a)$ and $\alpha_1(x,x',e_1a)$ satisfy the developed conditions by Eringen, the constitutive relation of the nonlocal strain gradient theory has the following form:

$$\left[1-(e_1a)^2\nabla^2\right]\left[1-(e_0a)^2\nabla^2\right]\sigma_{ij} = C_{ijkl}\left[1-(e_1a)^2\nabla^2\right]\varepsilon_{kl} - C_{ijkl}l^2\left[1-(e_0a)^2\nabla^2\right]\nabla^2\varepsilon_{kl}, \tag{3}$$

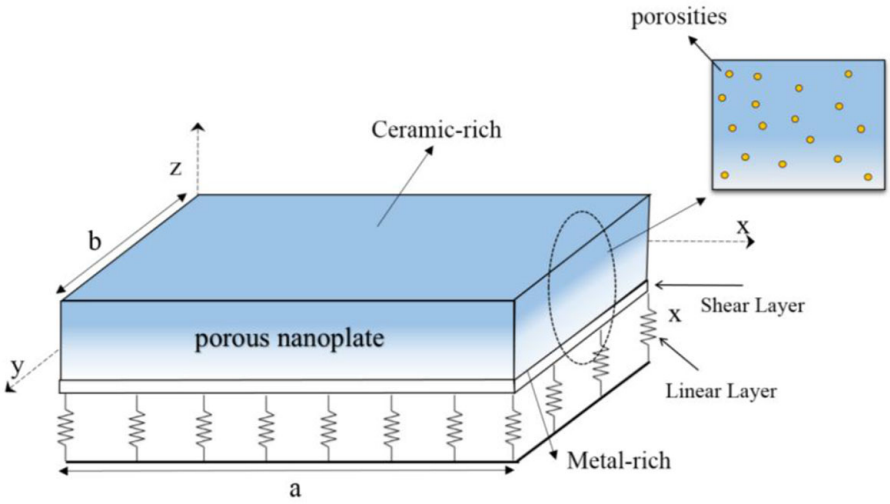

Fig. 1. Configuration of the nanoporous inhomogeneous nanoplate on the elastic substrate.

in which ∇^2 denotes the Laplacian operator. Considering $e_1 = e_0 = e$, the general constitutive relation in eq. (3) becomes

$$\left[1-(ea)^2\nabla^2\right]\sigma_{ij} = C_{ijkl}\left[1-l^2\nabla^2\right]\varepsilon_{kl}. \tag{4}$$

To consider hygro-thermal effects, eq. (4) can be written as [55]

$$\left[1-(ea)^2\nabla^2\right]\sigma_{ij} = C_{ijkl}\left[1-l^2\nabla^2\right](\varepsilon_{kl}-\gamma_{ij}T-\beta_{ij}C), \tag{5}$$

where γ_{ij} and β_{ij} are thermal and moisture expansion coefficients, respectively.

3 FG plate model based on neutral surface position

Consider a rectangular $(a \times b)$ porous nanoplate of uniform thickness h made of FGM, as shown in fig. 1. A FG material can be specified by the variation in the volume fractions. Due to this variation, the neutral axis of the FG nanoplate may not coincide with its mid-surface, which leads to bending-extension coupling. By using the neutral axis, this coupling is eliminated. Based on the modified power-law model, Young' modulus E, density ρ, thermal expansion coefficient γ and moisture expansion coefficient β are described as

$$E(z) = (E_c - E_m)\left(\frac{z}{h}+\frac{1}{2}\right)^p + E_m - \frac{\xi}{2}(E_c+E_m), \tag{6a}$$

$$\rho(z) = (\rho_c - \rho_m)\left(\frac{z}{h}+\frac{1}{2}\right)^p + \rho_m - \frac{\xi}{2}(\rho_c+\rho_m), \tag{6b}$$

$$\gamma(z) = (\gamma_c - \gamma_m)\left(\frac{z}{h}+\frac{1}{2}\right)^p + \gamma_m - \frac{\xi}{2}(\gamma_c+\gamma_m), \tag{6c}$$

$$\beta(z) = (\beta_c - \beta_m)\left(\frac{z}{h}+\frac{1}{2}\right)^p + \beta_m - \frac{\xi}{2}(\beta_c+\beta_m), \tag{6d}$$

in which c and m denote the material properties of ceramic and metal phases, respectively, and p is the inhomogeneity or power-law index. Also, ξ is the porosity volume fraction. The displacement field according to the four-variable plate model considering exact position of neutral surface can be expressed by

$$u_1(x,y,z,t) = u(x,y,t) - (z-z^*)\frac{\partial w_b}{\partial x} - [f(z)-z^{**}]\frac{\partial w_s}{\partial x}, \tag{7a}$$

$$u_2(x,y,z,t) = v(x,y,t) - (z-z^*)\frac{\partial w_b}{\partial y} - [f(z)-z^{**}]\frac{\partial w_s}{\partial y}, \tag{7b}$$

$$u_3(x,y,z,t) = w(x,y,t) = w_b(x,y,t) + w_s(x,y,t), \tag{7c}$$

where

$$z^* = \frac{\int_{-h/2}^{h/2} E(z)\, z \mathrm{d}z}{\int_{-h/2}^{h/2} E(z)\, \mathrm{d}z}\,,$$

$$z^{**} = \frac{\int_{-h/2}^{h/2} E(z)\, f(z) \mathrm{d}z}{\int_{-h/2}^{h/2} E(z)\, \mathrm{d}z}\,. \tag{8}$$

Also, u and v are in-plane displacements and w_b and w_s denote the bending and shear transverse displacement, respectively. The shape function of transverse shear deformation is considered as

$$f(z) = -\frac{z}{4} + \frac{5z^3}{3h^2}\,. \tag{9}$$

According to the present plate theory with four unknowns, the nonzero strains are obtained as

$$\begin{aligned}
\varepsilon_x &= \frac{\partial u}{\partial x} - (z - z^*)\frac{\partial^2 w_b}{\partial x^2} - [f(z) - z^{**}]\frac{\partial^2 w_s}{\partial x^2}\,,\\
\varepsilon_y &= \frac{\partial v}{\partial y} - (z - z^*)\frac{\partial^2 w_b}{\partial y^2} - [f(z) - z^{**}]\frac{\partial^2 w_s}{\partial y^2}\,,\\
\gamma_{xy} &= \frac{\partial u}{\partial y} + \frac{\partial v}{\partial x} - 2(z - z^*)\frac{\partial^2 w_b}{\partial x \partial y} - 2[f(z) - z^{**}]\frac{\partial^2 w_s}{\partial x \partial y}\,,\\
\gamma_{yz} &= g(z)\frac{\partial w_s}{\partial y}\,, \qquad \gamma_{xz} = g(z)\frac{\partial w_s}{\partial x}\,.
\end{aligned} \tag{10}$$

Also, the extended Hamilton's principle expresses that

$$\int_0^t \delta(U - T + V)\, \mathrm{d}t = 0. \tag{11}$$

Here, U is strain energy, T is kinetic energy and V is work done by external forces. The first variation of the strain energy can be calculated as

$$\begin{aligned}
\delta U = \int_V \Big(&\sigma_{xx}\delta\varepsilon_{xx} + \sigma^{(1)}_{xx}\delta\nabla\varepsilon_{xx} + \sigma_{yy}\delta\varepsilon_{yy} + \sigma^{(1)}_{yy}\delta\nabla\varepsilon_{yy} + \sigma_{xy}\delta\gamma_{xy} + \sigma^{(1)}_{xy}\delta\nabla\gamma_{xy}\\
&+ \sigma_{yz}\delta\gamma_{yz} + \sigma^{(1)}_{yz}\delta\nabla\gamma_{yz} + \sigma_{xz}\delta\gamma_{xz} + \sigma^{(1)}_{xz}\delta\nabla\gamma_{xz}\Big)\, \mathrm{d}V,
\end{aligned} \tag{12}$$

in which σ_{ij} are the components of the stress tensor and ε_{ij} are the components of the strain tensor.

Substituting eqs. (8) and (10) into eq. (12) yields

$$\begin{aligned}
\delta U = \int_0^a \int_0^b \Bigg[&N_{xx}\left[\frac{\partial \delta u}{\partial x} + \frac{\partial w}{\partial x}\frac{\partial \delta w}{\partial x}\right] - M^b_{xx}\frac{\partial^2 \delta w_b}{\partial x^2} - M^s_{xx}\frac{\partial^2 \delta w_s}{\partial x^2} + N_{yy}\left[\frac{\partial \delta v}{\partial y} + \frac{\partial w}{\partial y}\frac{\partial \delta w}{\partial y}\right]\\
&- M^b_{yy}\frac{\partial^2 \delta w_b}{\partial y^2} - M^s_{yy}\frac{\partial^2 \delta w_s}{\partial y^2} + N_{xy}\left(\frac{\partial \delta u}{\partial y} + \frac{\partial \delta v}{\partial x} + \frac{\partial w}{\partial x}\frac{\partial \delta w}{\partial y} + \frac{\partial w}{\partial y}\frac{\partial \delta w}{\partial x}\right) - 2M^b_{xy}\frac{\partial^2 \delta w_b}{\partial x \partial y}\\
&- 2M^s_{xy}\frac{\partial^2 \delta w_s}{\partial x \partial y} + Q_{yz}\frac{\partial \delta w_s}{\partial y} + Q_{xz}\frac{\partial \delta w_s}{\partial x}\Bigg]\mathrm{d}y\, \mathrm{d}x,
\end{aligned} \tag{13}$$

in which

$$
\begin{aligned}
N_{xx} &= \int_{-h/2}^{h/2} \left(\sigma_{xx}^{0} - \nabla\sigma_{xx}^{(1)}\right) \mathrm{d}z = N_{xx}^{(0)} - \nabla N_{xx}^{(1)},\\
N_{xy} &= \int_{-h/2}^{h/2} \left(\sigma_{xy}^{0} - \nabla\sigma_{xy}^{(1)}\right) \mathrm{d}z = N_{xy}^{(0)} - \nabla N_{xy}^{(1)},\\
N_{yy} &= \int_{-h/2}^{h/2} \left(\sigma_{yy}^{0} - \nabla\sigma_{yy}^{(1)}\right) \mathrm{d}z = N_{yy}^{(0)} - \nabla N_{yy}^{(1)},\\
M_{xx}^{b} &= \int_{-h/2}^{h/2} z\left(\sigma_{xx}^{0} - \nabla\sigma_{xx}^{(1)}\right) \mathrm{d}z = M_{xx}^{b(0)} - \nabla M_{xx}^{b(1)},\\
M_{xx}^{s} &= \int_{-h/2}^{h/2} f\left(\sigma_{xx}^{0} - \nabla\sigma_{xx}^{(1)}\right) \mathrm{d}z = M_{xx}^{s(0)} - \nabla M_{xx}^{s(1)},\\
M_{yy}^{b} &= \int_{-h/2}^{h/2} z\left(\sigma_{yy}^{0} - \nabla\sigma_{yy}^{(1)}\right) \mathrm{d}z = M_{yy}^{b(0)} - \nabla M_{yy}^{b(1)},\\
M_{yy}^{s} &= \int_{-h/2}^{h/2} f\left(\sigma_{yy}^{0} - \nabla\sigma_{yy}^{(1)}\right) \mathrm{d}z = M_{yy}^{s(0)} - \nabla M_{yy}^{s(1)},\\
M_{xy}^{b} &= \int_{-h/2}^{h/2} z\left(\sigma_{xy}^{0} - \nabla\sigma_{xy}^{(1)}\right) \mathrm{d}z = M_{xy}^{b(0)} - \nabla M_{xy}^{b(1)},\\
M_{xy}^{s} &= \int_{-h/2}^{h/2} f\left(\sigma_{xy}^{0} - \nabla\sigma_{xy}^{(1)}\right) \mathrm{d}z = M_{xy}^{s(0)} - \nabla M_{xy}^{s(1)},\\
Q_{xz} &= \int_{-h/2}^{h/2} g\left(\sigma_{xz}^{0} - \nabla\sigma_{xz}^{(1)}\right) \mathrm{d}z = Q_{xz}^{(0)} - \nabla Q_{xz}^{(1)},\\
Q_{yz} &= \int_{-h/2}^{h/2} g\left(\sigma_{yz}^{0} - \nabla\sigma_{yz}^{(1)}\right) \mathrm{d}z = Q_{yz}^{(0)} - \nabla Q_{yz}^{(1)},
\end{aligned}
\tag{14a}
$$

where

$$
\begin{aligned}
N_{ij}^{(0)} &= \int_{-h/2}^{h/2} \left(\sigma_{ij}^{(0)}\right) \mathrm{d}z, \qquad N_{ij}^{(1)} = \int_{-h/2}^{h/2} \left(\sigma_{ij}^{(1)}\right) \mathrm{d}z,\\
M_{ij}^{b(0)} &= \int_{-h/2}^{h/2} z\left(\sigma_{ij}^{b(0)}\right) \mathrm{d}z, \qquad M_{ij}^{b(1)} = \int_{-h/2}^{h/2} z\left(\sigma_{ij}^{b(1)}\right) \mathrm{d}z,\\
M_{ij}^{s(0)} &= \int_{-h/2}^{h/2} f\left(\sigma_{ij}^{s(0)}\right) \mathrm{d}z, \qquad M_{ij}^{s(1)} = \int_{-h/2}^{h/2} f\left(\sigma_{ij}^{s(1)}\right) \mathrm{d}z,\\
Q_{xz}^{(0)} &= \int_{-h/2}^{h/2} g\left(\sigma_{xz}^{i(0)}\right) \mathrm{d}z, \qquad Q_{xz}^{(1)} = \int_{-h/2}^{h/2} g\left(\sigma_{xz}^{i(1)}\right) \mathrm{d}z,\\
Q_{yz}^{(0)} &= \int_{-h/2}^{h/2} g\left(\sigma_{yz}^{i(0)}\right) \mathrm{d}z, \qquad Q_{yz}^{(1)} = \int_{-h/2}^{h/2} g\left(\sigma_{yz}^{i(1)}\right) \mathrm{d}z,
\end{aligned}
\tag{14b}
$$

in which $(ij = xx, xy, yy)$. The first variation of the work done by applied forces can be written as:

$$
\begin{aligned}
\delta V = \int_0^a \int_0^b \Bigg(& N_x^0 \frac{\partial(w_b + w_s)}{\partial x} \frac{\partial\delta(w_b + w_s)}{\partial x} + N_y^0 \frac{\partial(w_b + w_s)}{\partial y} \frac{\partial\delta(w_b + w_s)}{\partial y}\\
& + 2\delta N_{xy}^0 \frac{\partial(w_b + w_s)}{\partial x} \frac{\partial(w_b + w_s)}{\partial y} - k_w(w_b + w_s)\delta(w_b + w_s)\\
& + k_p \left(\frac{\partial(w_b + w_s)}{\partial x} \frac{\partial\delta(w_b + w_s)}{\partial x} + \frac{\partial(w_b + w_s)}{\partial y} \frac{\partial\delta(w_b + w_s)}{\partial y} \right) \Bigg) \mathrm{d}y\, \mathrm{d}x,
\end{aligned}
\tag{15}
$$

where N_x^0, N_y^0, N_{xy}^0 are in-plane applied loads, k_w and k_p are Winkler and Pasternak constants. The first variation of the kinetic energy can be written in the following form:

$$\begin{aligned}\delta K = \int_0^a \int_0^b \Bigg[& I_0 \left(\frac{\partial u}{\partial t}\frac{\partial \delta u}{\partial t} + \frac{\partial v}{\partial t}\frac{\partial \delta v}{\partial t} + \frac{\partial (w_b + w_s)}{\partial t}\frac{\partial \delta (w_b + w_s)}{\partial t} \right) - I_1 \left(\frac{\partial u}{\partial t}\frac{\partial \delta w_b}{\partial x \partial t} + \frac{\partial w_b}{\partial x \partial t}\frac{\partial \delta u}{\partial t} + \frac{\partial v}{\partial t}\frac{\partial \delta w_b}{\partial y \partial t} + \frac{\partial w_b}{\partial y \partial t}\frac{\partial \delta v}{\partial t} \right) \\ & - I_3 \left(\frac{\partial u}{\partial t}\frac{\partial \delta w_s}{\partial x \partial t} + \frac{\partial w_s}{\partial x \partial t}\frac{\partial \delta u}{\partial t} + \frac{\partial v}{\partial t}\frac{\partial \delta w_s}{\partial y \partial t} + \frac{\partial w_s}{\partial y \partial t}\frac{\partial \delta v}{\partial t} \right) + I_2 \left(\frac{\partial w_b}{\partial x \partial t}\frac{\partial \delta w_b}{\partial x \partial t} + \frac{\partial w_b}{\partial y \partial t}\frac{\partial \delta w_b}{\partial y \partial t} \right) \\ & + I_5 \left(\frac{\partial w_s}{\partial x \partial t}\frac{\partial \delta w_s}{\partial x \partial t} + \frac{\partial w_s}{\partial y \partial t}\frac{\partial \delta w_s}{\partial y \partial t} \right) + I_4 \left(\frac{\partial w_b}{\partial x \partial t}\frac{\partial \delta w_s}{\partial x \partial t} + \frac{\partial w_s}{\partial x \partial t}\frac{\partial \delta w_b}{\partial x \partial t} + \frac{\partial w_b}{\partial y \partial t}\frac{\partial \delta w_s}{\partial y \partial t} + \frac{\partial w_s}{\partial y \partial t}\frac{\partial \delta w_b}{\partial y \partial t} \right) \Bigg] \mathrm{d}y\, \mathrm{d}x, \end{aligned} \tag{16}$$

in which

$$(I_0, I_1, I_2, I_3, I_4, I_5) = \int_{-h/2}^{h/2} \left(1, z - z^*, (z - z^*)^2, f - z^{**}, (z - z^*)(f - z^{**}), (f - z^{**})^2\right) \rho(z) \mathrm{d}z. \tag{17}$$

By inserting eqs. (13)–(16) into eq. (11) and setting the coefficients of δu, δv, δw_b and δw_s to zero, the following Euler-Lagrange equations can be obtained:

$$\frac{\partial N_x}{\partial x} + \frac{\partial N_{xy}}{\partial y} = I_0 \frac{\partial^2 u}{\partial t^2} - I_1 \frac{\partial^3 w_b}{\partial x \partial t^2} - I_3 \frac{\partial^3 w_s}{\partial x \partial t^2}, \tag{18}$$

$$\frac{\partial N_{xy}}{\partial x} + \frac{\partial N_y}{\partial y} = I_0 \frac{\partial^2 v}{\partial t^2} - I_1 \frac{\partial^3 w_b}{\partial y \partial t^2} - I_3 \frac{\partial^3 w_s}{\partial y \partial t^2}, \tag{19}$$

$$\begin{aligned} & \frac{\partial^2 M_x^b}{\partial x^2} + 2\frac{\partial^2 M_{xy}^b}{\partial x \partial y} + \frac{\partial^2 M_y^b}{\partial y^2} - (N^T + N^H + N^0)\nabla^2 (w_b + w_s) - k_w (w_b + w_s) + k_p \nabla^2 (w_b + w_s) = \\ & + I_0 \frac{\partial^2 (w_b + w_s)}{\partial t^2} + I_1 \left(\frac{\partial^3 u}{\partial x \partial t^2} + \frac{\partial^3 v}{\partial y \partial t^2} \right) - I_2 \nabla^2 \left(\frac{\partial^2 w_b}{\partial t^2} \right) - I_4 \nabla^2 \left(\frac{\partial^2 w_s}{\partial t^2} \right), \end{aligned} \tag{20}$$

$$\begin{aligned} & \frac{\partial^2 M_x^s}{\partial x^2} + 2\frac{\partial^2 M_{xy}^s}{\partial x \partial y} + \frac{\partial^2 M_y^s}{\partial y^2} + \frac{\partial Q_{xz}}{\partial x} + \frac{\partial Q_{yz}}{\partial y} - (N^T + N^H + N^0)\nabla^2 (w_b + w_s) - k_w (w_b + w_s) \\ & + k_p \nabla^2 (w_b + w_s) = + I_0 \frac{\partial^2 (w_b + w_s)}{\partial t^2} + I_3 \left(\frac{\partial^3 u}{\partial x \partial t^2} + \frac{\partial^3 v}{\partial y \partial t^2} \right) - I_4 \nabla^2 \left(\frac{\partial^2 w_b}{\partial t^2} \right) - I_5 \nabla^2 \left(\frac{\partial^2 w_s}{\partial t^2} \right), \end{aligned} \tag{21}$$

where $N_x^0 = N_y^0 = N^T + N^H + N^0$, $N_{xy}^0 = 0$ and the hygro-thermal resultant can be expressed by

$$\begin{aligned} N^T &= \int_{-h/2}^{h/2} \frac{E(z)}{1 - v} \gamma(z)(T - T_0) \mathrm{d}z, \\ N^H &= \int_{-h/2}^{h/2} \frac{E(z)}{1 - v} \beta(z)(C - C_0) \mathrm{d}z, \end{aligned} \tag{22}$$

in which $C = \Delta C + C_0$ and $T = \Delta T + T_0$ are uniform moisture and temperature changes; C_0 and T_0 are reference moisture and temperature.

The classical and nonclassical boundary conditions can be obtained in the derivation process when using the integrations by parts. The nonclassical boundary conditions are

$$\begin{aligned} &\text{Specify} \quad \frac{\partial^2 w_b}{\partial x^2} \quad \text{or} \quad M_{xx}^{b(1)} = 0, \\ &\text{Specify} \quad \frac{\partial^2 w_b}{\partial y^2} \quad \text{or} \quad M_{yy}^{b(1)} = 0, \\ &\text{Specify} \quad \frac{\partial^2 w_s}{\partial x^2} \quad \text{or} \quad M_{xx}^{s(1)} = 0, \\ &\text{Specify} \quad \frac{\partial^2 w_s}{\partial y^2} \quad \text{or} \quad M_{yy}^{s(1)} = 0. \end{aligned} \tag{23}$$

Based on the NSGT, the constitutive relations of presented higher-order FG nanoplate can be stated as

$$(1-\mu\nabla^2)\begin{Bmatrix}\sigma_x\\ \sigma_y\\ \sigma_{xy}\\ \sigma_{yz}\\ \sigma_{xz}\end{Bmatrix}=\frac{E(z)}{1-v^2}(1-\lambda\nabla^2)\begin{pmatrix}1 & v & 0 & 0 & 0\\ v & 1 & 0 & 0 & 0\\ 0 & 0 & (1-v)/2 & 0 & 0\\ 0 & 0 & 0 & (1-v)/2 & 0\\ 0 & 0 & 0 & 0 & (1-v)/2\end{pmatrix}\begin{Bmatrix}\varepsilon_x-\gamma\Delta T-\beta\Delta C\\ \varepsilon_y-\gamma\Delta T-\beta\Delta C\\ \gamma_{xy}\\ \gamma_{yz}\\ \gamma_{xz}\end{Bmatrix}. \tag{24}$$

Integrating eq. (24) over the plate's cross-section area, one can obtain the force strain and the moment strain of the nonlocal refined FG plates as follows:

$$(1-\mu\nabla^2)\begin{Bmatrix}N_x\\ N_y\\ N_{xy}\end{Bmatrix}=A(1-\lambda\nabla^2)\begin{pmatrix}1 & v & 0\\ v & 1 & 0\\ 0 & 0 & (1-v)/2\end{pmatrix}\begin{Bmatrix}\dfrac{\partial u}{\partial x}\\ \dfrac{\partial v}{\partial y}\\ \dfrac{\partial u}{\partial y}+\dfrac{\partial v}{\partial x}\end{Bmatrix}, \tag{25}$$

$$(1-\mu\nabla^2)\begin{Bmatrix}M_x^b\\ M_y^b\\ M_{xy}^b\end{Bmatrix}=D(1-\lambda\nabla^2)\begin{pmatrix}1 & v & 0\\ v & 1 & 0\\ 0 & 0 & (1-v)/2\end{pmatrix}\begin{Bmatrix}-\dfrac{\partial^2 w_b}{\partial x^2}\\ -\dfrac{\partial^2 w_b}{\partial y^2}\\ -2\dfrac{\partial^2 w_b}{\partial x\partial y}\end{Bmatrix}+E(1-\lambda\nabla^2)\begin{pmatrix}1 & v & 0\\ v & 1 & 0\\ 0 & 0 & (1-v)/2\end{pmatrix}\begin{Bmatrix}-\dfrac{\partial^2 w_s}{\partial x^2}\\ -\dfrac{\partial^2 w_s}{\partial y^2}\\ -2\dfrac{\partial^2 w_s}{\partial x\partial y}\end{Bmatrix}, \tag{26}$$

$$(1-\mu\nabla^2)\begin{Bmatrix}M_x^s\\ M_y^s\\ M_{xy}^s\end{Bmatrix}=E(1-\lambda\nabla^2)\begin{pmatrix}1 & v & 0\\ v & 1 & 0\\ 0 & 0 & (1-v)/2\end{pmatrix}\begin{Bmatrix}-\dfrac{\partial^2 w_b}{\partial x^2}\\ -\dfrac{\partial^2 w_b}{\partial y^2}\\ -2\dfrac{\partial^2 w_b}{\partial x\partial y}\end{Bmatrix}+F(1-\lambda\nabla^2)\begin{pmatrix}1 & v & 0\\ v & 1 & 0\\ 0 & 0 & (1-v)/2\end{pmatrix}\begin{Bmatrix}-\dfrac{\partial^2 w_s}{\partial x^2}\\ -\dfrac{\partial^2 w_s}{\partial y^2}\\ -2\dfrac{\partial^2 w_s}{\partial x\partial y}\end{Bmatrix}, \tag{27}$$

$$(1-\mu\nabla^2)\begin{Bmatrix}Q_x\\ Q_y\end{Bmatrix}=A_{44}(1-\lambda\nabla^2)\begin{pmatrix}1 & 0\\ 0 & 1\end{pmatrix}\begin{Bmatrix}\dfrac{\partial w_s}{\partial x}\\ \dfrac{\partial w_s}{\partial y}\end{Bmatrix}, \tag{28}$$

in which

$$\begin{aligned}A&=\int_{-h/2}^{h/2}\frac{E(z)}{1-v^2}\mathrm{d}z,\\ D&=\int_{-h/2}^{h/2}\frac{E(z)(z-z^*)^2}{1-v^2}\mathrm{d}z,\\ E&=\int_{-h/2}^{h/2}\frac{E(z)(z-z^*)(f-z^{**})}{1-v^2}\mathrm{d}z,\\ F&=\int_{-h/2}^{h/2}\frac{E(z)(f-z^{**})^2}{1-v^2}\mathrm{d}z,\\ A_{44}&=\int_{-h/2}^{h/2}\frac{E(z)}{2(1+v)}g^2\mathrm{d}z.\end{aligned} \tag{29}$$

The governing equations in terms of the displacements for a NSGT refined four-variable FG nanoplate can be derived by substituting eqs. (25)–(28), into eqs. (18)–(21) as follows:

$$A(1-\lambda\nabla^2)\left(\frac{\partial^2 u}{\partial x^2}+\frac{1-v}{2}\frac{\partial^2 u}{\partial y^2}+\frac{1+v}{2}\frac{\partial^2 v}{\partial x\partial y}\right)+(1-\mu\nabla^2)\left(-I_0\frac{\partial^2 u}{\partial t^2}+I_1\frac{\partial^3 w_b}{\partial x\partial t^2}+I_3\frac{\partial^3 w_s}{\partial x\partial t^2}\right)=0, \tag{30}$$

$$A(1-\lambda\nabla^2)\left(\frac{\partial^2 v}{\partial y^2}+\frac{1-v}{2}\frac{\partial^2 v}{\partial x^2}+\frac{1+v}{2}\frac{\partial^2 u}{\partial x\partial y}\right)+(1-\mu\nabla^2)\left(-I_0\frac{\partial^2 v}{\partial t^2}+I_1\frac{\partial^3 w_b}{\partial y\partial t^2}+I_3\frac{\partial^3 w_s}{\partial y\partial t^2}\right)=0, \tag{31}$$

$$\begin{aligned}&-D(1-\lambda\nabla^2)\left(\frac{\partial^4 w_b}{\partial x^4}+2\frac{\partial^4 w_b}{\partial x^2\partial y^2}+\frac{\partial^4 w_b}{\partial y^4}\right)-E(1-\lambda\nabla^2)\left(\frac{\partial^4 w_s}{\partial x^4}+2\frac{\partial^4 w_s}{\partial x^2\partial y^2}+\frac{\partial^4 w_s}{\partial y^4}\right)\\&+(1-\mu\nabla^2)\Bigg(-I_0\frac{\partial^2(w_b+w_s)}{\partial t^2}-I_1\left(\frac{\partial^3 u}{\partial x\partial t^2}+\frac{\partial^3 v}{\partial y\partial t^2}\right)+I_2\nabla^2\left(\frac{\partial^2 w_b}{\partial t^2}\right)\\&+I_4\nabla^2\left(\frac{\partial^2 w_s}{\partial t^2}\right)-(N^T+N^H+N^0)\nabla^2(w_b+w_s)-k_w(w_b+w_s)+k_p\nabla^2(w_b+w_s)\Bigg)=0,\end{aligned} \tag{32}$$

$$\begin{aligned}&-E(1-\lambda\nabla^2)\left(\frac{\partial^4 w_b}{\partial x^4}+2\frac{\partial^4 w_b}{\partial x^2\partial y^2}+\frac{\partial^4 w_b}{\partial y^4}\right)-F(1-\lambda\nabla^2)\left(\frac{\partial^4 w_s}{\partial x^4}+2\frac{\partial^4 w_s}{\partial x^2\partial y^2}+\frac{\partial^4 w_s}{\partial y^4}\right)\\&+A_{44}(1-\lambda\nabla^2)\left(\frac{\partial^2 w_s}{\partial x^2}+\frac{\partial^2 w_s}{\partial y^2}\right)+(1-\mu\nabla^2)\Bigg(-I_0\frac{\partial^2(w_b+w_s)}{\partial t^2}-I_3\left(\frac{\partial^3 u}{\partial x\partial t^2}+\frac{\partial^3 v}{\partial y\partial t^2}\right)\\&+I_4\nabla^2\left(\frac{\partial^2 w_b}{\partial t^2}\right)+I_5\nabla^2\left(\frac{\partial^2 w_s}{\partial t^2}\right)-(N^T+N^H+N^0)\nabla^2(w_b+w_s)-k_w(w_b+w_s)+k_p\nabla^2(w_b+w_s)\Bigg)=0.\end{aligned} \tag{33}$$

4 Solution procedure

In this section, Galerkin's method is implemented to solve the governing equations of nonlocal strain gradient based FG nanoplates. Thus, the displacement field can be calculated as

$$u=\sum_{m=1}^{\infty}\sum_{n=1}^{\infty}U_{mn}\frac{\partial X_m(x)}{\partial x}Y_n(y)e^{i\omega_n t}, \tag{34}$$

$$v=\sum_{m=1}^{\infty}\sum_{n=1}^{\infty}V_{mn}X_m(x)\frac{\partial Y_n(y)}{\partial y}e^{i\omega_n t}, \tag{35}$$

$$w_b=\sum_{m=1}^{\infty}\sum_{n=1}^{\infty}W_{bmn}X_m(x)Y_n(y)e^{i\omega_n t}, \tag{36}$$

$$w_s=\sum_{m=1}^{\infty}\sum_{n=1}^{\infty}W_{smn}X_m(x)Y_n(y)e^{i\omega_n t}, \tag{37}$$

where (U_{mn}, V_{mn}, W_{bmn}, W_{smn}) are the unknown coefficients and the functions X_m and Y_n satisfy the boundary conditions. The classical and nonclassical boundary condition based on the present plate model are

$$\begin{aligned}&w_b=w_s=0,\\&\frac{\partial^2 w_b}{\partial x^2}=\frac{\partial^2 w_s}{\partial x^2}=\frac{\partial^2 w_b}{\partial y^2}=\frac{\partial^2 w_s}{\partial y^2}=0,\\&\frac{\partial^4 w_b}{\partial x^4}=\frac{\partial^4 w_s}{\partial x^4}=\frac{\partial^4 w_b}{\partial y^4}=\frac{\partial^4 w_s}{\partial y^4}=0.\end{aligned} \tag{38}$$

By substituting eqs. (34)–(37) into eqs. (30)–(33), the matrix form of the governing equations of harmonically loaded nanoplate can be expressed by

$$[M]\{\ddot{\Lambda}\}+[[K]+N_0(t)[G]]\{\Lambda\}=0, \tag{39}$$

where [**M**], [**K**] and [**G**] denote the mass, stiffness and geometric stiffness matrices, respectively, and $\{\Lambda\}$ is the displacement vector ($\{\Lambda\}=\{U_{mn},V_{mn},W_{bmn},W_{smn}\}$).

Considering the periodic axial excitation compressive load $N_0(t)=-[\alpha+\beta\cos(\varpi t)]N_{cr}$, which consists of static and dynamical components, the governing equation can be expressed by

$$[M]\{\ddot{\Lambda}\}+[[K]-\{\alpha+\beta\cos(\varpi t)\}N_{cr}[G]]\{\Lambda\}=0, \tag{40}$$

where ϖ and N_{cr} denote excitation frequency and buckling load, respectively, α and β denote the static and dynamic load factors. To calculate dimensionless excitation frequency, the following relation is adopted:

$$\Omega = \varpi a \sqrt{\frac{\rho_c}{E_c}}\,. \tag{41}$$

The instability boundaries considering periodic coefficients of the Mathieu-Hill type can be formed by periodic T_0 and $2T_0$, in which $T_0 = 2\pi/\varpi$. It is reported that the boundaries of instability regions with period T_0 are less important compared to those with period $2T_0$. The solution with respect to period $2T_0$ can be obtained by the following equation:

$$[[K] - N_{cr}\{\alpha \pm 0.5\beta\}[G] - 0.25\varpi[M]]\{\Lambda\} = 0. \tag{42}$$

The nontrivial solution of eq. (20) gives

$$\det \begin{vmatrix} [\bar{K}] - (0.5\beta)N_{cr}[G] - (0.25\varpi)[M] & 0 \\ 0 & [\bar{K}] + (0.5\beta)N_{cr}[G] - (0.25\varpi)[M] \end{vmatrix} = 0, \tag{43}$$

in which $[\bar{K}] = [K] - \alpha N_{cr}[G]$. For a given value of α, the plots of eigenfrequency Ω with respect to β provide stability regions of the nonlocal FGM nanoplates.

Also, the components of stiffness and mass matrices are expressed by

$$\begin{aligned} k_{1,1} = A\Bigg(& \int_0^b \int_0^a \left(\frac{\partial^3 X_m}{\partial x^3} Y_n \frac{\partial X_m}{\partial x} Y_n \right) \mathrm{d}x\,\mathrm{d}y - \lambda \Bigg(\int_0^b \int_0^a \left(\frac{\partial^5 X_m}{\partial x^5} Y_n \frac{\partial X_m}{\partial x} Y_n \right) \mathrm{d}x\,\mathrm{d}y \\ & + \int_0^b \int_0^a \left(\frac{\partial^3 X_m}{\partial x^3} \frac{\partial^2 Y_n}{\partial y^2} \frac{\partial X_m}{\partial x} Y_n \right) \mathrm{d}x\,\mathrm{d}y \Bigg) \Bigg) + A \frac{1-v}{2} \Bigg(\int_0^b \int_0^a \left(\frac{\partial X_m}{\partial x} \frac{\partial^2 Y_n}{\partial y^2} \frac{\partial X_m}{\partial x} Y_n \right) \mathrm{d}x\,\mathrm{d}y \\ & - \lambda \Bigg(\int_0^b \int_0^a \left(\frac{\partial^3 X_m}{\partial x^3} \frac{\partial^2 Y_n}{\partial y^2} \frac{\partial X_m}{\partial x} Y_n \right) \mathrm{d}x\,\mathrm{d}y + \int_0^b \int_0^a \left(\frac{\partial X_m}{\partial x} \frac{\partial^4 Y_n}{\partial y^4} \frac{\partial X_m}{\partial x} Y_n \right) \mathrm{d}x\,\mathrm{d}y \Bigg) \Bigg), \end{aligned} \tag{44}$$

$$\begin{aligned} k_{1,2} = A\frac{1+v}{2}\Bigg(& \int_0^b \int_0^a \left(\frac{\partial^2 X_m}{\partial x^2} \frac{\partial Y_n}{\partial y} X_m \frac{\partial Y_n}{\partial y} \right) \mathrm{d}x\,\mathrm{d}y - \lambda \Bigg(\int_0^b \int_0^a \left(\frac{\partial^4 X_m}{\partial x^4} \frac{\partial Y_n}{\partial y} X_m \frac{\partial Y_n}{\partial y} \right) \mathrm{d}x\,\mathrm{d}y \\ & + \int_0^b \int_0^a \left(\frac{\partial^2 X_m}{\partial x^2} \frac{\partial^3 Y_n}{\partial y^3} X_m \frac{\partial Y_n}{\partial y} \right) \mathrm{d}x\,\mathrm{d}y \Bigg) \Bigg), \end{aligned} \tag{45}$$

$$\begin{aligned} k_{2,1} = A\frac{1+v}{2}\Bigg(& \int_0^b \int_0^a \left(\frac{\partial X_m}{\partial x} \frac{\partial^2 Y_n}{\partial y^2} \frac{\partial X_m}{\partial x} Y_n \right) \mathrm{d}x\,\mathrm{d}y - \lambda \Bigg(\int_0^b \int_0^a \left(\frac{\partial^3 X_m}{\partial x^3} \frac{\partial^2 Y_n}{\partial y^2} \frac{\partial X_m}{\partial x} Y_n \right) \mathrm{d}x\,\mathrm{d}y \\ & + \int_0^b \int_0^a \left(\frac{\partial X_m}{\partial x} \frac{\partial^4 Y_n}{\partial y^4} \frac{\partial X_m}{\partial x} Y_n \right) \mathrm{d}x\,\mathrm{d}y \Bigg) \Bigg), \end{aligned} \tag{46}$$

$$\begin{aligned} k_{2,2} = A\Bigg(& \int_0^b \int_0^a \left(X_m \frac{\partial^3 Y_n}{\partial y^3} X_m \frac{\partial Y_n}{\partial y} \right) \mathrm{d}x\,\mathrm{d}y - \lambda \Bigg(\int_0^b \int_0^a \left(\frac{\partial^2 X_m}{\partial x^2} \frac{\partial^3 Y_n}{\partial y^3} X_m \frac{\partial Y_n}{\partial y} \right) \mathrm{d}x\,\mathrm{d}y \\ & + \int_0^b \int_0^a \left(X_m \frac{\partial^5 Y_n}{\partial y^5} X_m \frac{\partial Y_n}{\partial y} \right) \mathrm{d}x\,\mathrm{d}y \Bigg) \Bigg) + A \frac{1-v}{2} \Bigg(\int_0^b \int_0^a \left(\frac{\partial^2 X_m}{\partial x^2} \frac{\partial Y_n}{\partial y} X_m \frac{\partial Y_n}{\partial y} \right) \mathrm{d}x\,\mathrm{d}y \\ & - \lambda \Bigg(\int_0^b \int_0^a \left(\frac{\partial^4 X_m}{\partial x^4} \frac{\partial Y_n}{\partial y} X_m \frac{\partial Y_n}{\partial y} \right) \mathrm{d}x\,\mathrm{d}y + \int_0^b \int_0^a \left(\frac{\partial^2 X_m}{\partial x^2} \frac{\partial^3 Y_n}{\partial y^3} X_m \frac{\partial Y_n}{\partial y} \right) \mathrm{d}x\,\mathrm{d}y \Bigg) \Bigg), \end{aligned} \tag{47}$$

$$k_{2,3}=k_{3,2}=-E\Bigg(\int_0^b\int_0^a\left(\frac{\partial^4X_m}{\partial x^4}Y_nX_mY_n\right)\mathrm{d}x\,\mathrm{d}y+2\int_0^b\int_0^a\left(\frac{\partial^2X_m}{\partial x^2}\frac{\partial^2Y_n}{\partial y^2}X_mY_n\right)\mathrm{d}x\,\mathrm{d}y$$
$$+\int_0^b\int_0^a\left(X_m\frac{\partial^4Y_n}{\partial y^4}X_mY_n\right)\mathrm{d}x\,\mathrm{d}y-\lambda\Bigg(\int_0^b\int_0^a\left(\frac{\partial^6X_m}{\partial x^6}Y_nX_mY_n\right)\mathrm{d}x\,\mathrm{d}y$$
$$+3\int_0^b\int_0^a\left(\frac{\partial^4X_m}{\partial x^4}\frac{\partial^2Y_n}{\partial y^2}X_mY_n\right)\mathrm{d}x\,\mathrm{d}y+3\int_0^b\int_0^a\left(\frac{\partial^2X_m}{\partial x^2}\frac{\partial^4Y_n}{\partial y^4}X_mY_n\right)\mathrm{d}x\,\mathrm{d}y+\int_0^b\int_0^a\left(X_m\frac{\partial^6Y_n}{\partial y^6}X_mY_n\right)\mathrm{d}x\,\mathrm{d}y\Bigg)\Bigg),\quad(48)$$

$$k_{3,3}=-D\Bigg(\int_0^b\int_0^a\left(\frac{\partial^4X_m}{\partial x^4}Y_nX_mY_n\right)\mathrm{d}x\,\mathrm{d}y+2\int_0^b\int_0^a\left(\frac{\partial^2X_m}{\partial x^2}\frac{\partial^2Y_n}{\partial y^2}X_mY_n\right)\mathrm{d}x\,\mathrm{d}y$$
$$+\int_0^b\int_0^a\left(X_m\frac{\partial^4Y_n}{\partial y^4}X_mY_n\right)\mathrm{d}x\,\mathrm{d}y-\lambda\Bigg(\int_0^b\int_0^a\left(\frac{\partial^6X_m}{\partial x^6}Y_nX_mY_n\right)\mathrm{d}x\,\mathrm{d}y$$
$$+3\int_0^b\int_0^a\left(\frac{\partial^4X_m}{\partial x^4}\frac{\partial^2Y_n}{\partial y^2}X_mY_n\right)\mathrm{d}x\,\mathrm{d}y+3\int_0^b\int_0^a\left(\frac{\partial^2X_m}{\partial x^2}\frac{\partial^4Y_n}{\partial y^4}X_mY_n\right)\mathrm{d}x\,\mathrm{d}y$$
$$+\int_0^b\int_0^a\left(X_m\frac{\partial^6Y_n}{\partial y^6}X_mY_n\right)\mathrm{d}x\,\mathrm{d}y\Bigg)\Bigg)-K_w\Bigg(\int_0^b\int_0^a(X_mY_nX_mY_n)\mathrm{d}x\,\mathrm{d}y$$
$$-\mu\Bigg(\int_0^b\int_0^a\left(\frac{\partial^2X_m}{\partial x^2}Y_nX_mY_n\right)\mathrm{d}x\,\mathrm{d}y+\int_0^b\int_0^a\left(X_m\frac{\partial^2Y_n}{\partial y^2}X_mY_n\right)\mathrm{d}x\,\mathrm{d}y\Bigg)\Bigg)$$
$$-(N^T+N^H+N^0-K_p)\Bigg(\int_0^b\int_0^a\left(\frac{\partial^2X_m}{\partial x^2}Y_nX_mY_n\right)\mathrm{d}x\,\mathrm{d}y+\int_0^b\int_0^a\left(X_m\frac{\partial^2Y_n}{\partial y^2}X_mY_n\right)\mathrm{d}x\,\mathrm{d}y$$
$$-\mu\Bigg(\int_0^b\int_0^a\left(\frac{\partial^4X_m}{\partial x^4}Y_nX_mY_n\right)\mathrm{d}x\,\mathrm{d}y+2\int_0^b\int_0^a\left(\frac{\partial^2X_m}{\partial x^2}\frac{\partial^2Y_n}{\partial y^2}X_mY_n\right)\mathrm{d}x\,\mathrm{d}y+\int_0^b\int_0^a\left(X_m\frac{\partial^4Y_n}{\partial y^4}X_mY_n\right)\mathrm{d}x\,\mathrm{d}y\Bigg)\Bigg),\quad(49)$$

$$k_{4,4}=-F\Bigg(\int_0^b\int_0^a\left(\frac{\partial^4X_m}{\partial x^4}Y_nX_mY_n\right)\mathrm{d}x\,\mathrm{d}y+2\int_0^b\int_0^a\left(\frac{\partial^2X_m}{\partial x^2}\frac{\partial^2Y_n}{\partial y^2}X_mY_n\right)\mathrm{d}x\,\mathrm{d}y$$
$$+\int_0^b\int_0^a\left(X_m\frac{\partial^4Y_n}{\partial y^4}X_mY_n\right)\mathrm{d}x\,\mathrm{d}y-\lambda\Bigg(\int_0^b\int_0^a\left(\frac{\partial^6X_m}{\partial x^6}Y_nX_mY_n\right)\mathrm{d}x\,\mathrm{d}y$$
$$+3\int_0^b\int_0^a\left(\frac{\partial^4X_m}{\partial x^4}\frac{\partial^2Y_n}{\partial y^2}X_mY_n\right)\mathrm{d}x\,\mathrm{d}y+3\int_0^b\int_0^a\left(\frac{\partial^2X_m}{\partial x^2}\frac{\partial^4Y_n}{\partial y^4}X_mY_n\right)\mathrm{d}x\,\mathrm{d}y$$
$$+\int_0^b\int_0^a\left(X_m\frac{\partial^6Y_n}{\partial y^6}X_mY_n\right)\mathrm{d}x\,\mathrm{d}y\Bigg)\Bigg)+A_{44}\Bigg(\int_0^b\int_0^a\left(\frac{\partial^2X_m}{\partial x^2}Y_nX_mY_n\right)\mathrm{d}x\,\mathrm{d}y$$
$$+\int_0^b\int_0^a\left(X_m\frac{\partial^2Y_n}{\partial y^2}X_mY_n\right)\mathrm{d}x\,\mathrm{d}y-\lambda\Bigg(\int_0^b\int_0^a\left(\frac{\partial^4X_m}{\partial x^4}Y_nX_mY_n\right)\mathrm{d}x\,\mathrm{d}y$$
$$+2\int_0^b\int_0^a\left(\frac{\partial^2X_m}{\partial x^2}\frac{\partial^2Y_n}{\partial y^2}X_mY_n\right)\mathrm{d}x\,\mathrm{d}y+\int_0^b\int_0^a\left(X_m\frac{\partial^4Y_n}{\partial y^4}X_mY_n\right)\mathrm{d}x\,\mathrm{d}y\Bigg)\Bigg)$$
$$-K_w\Bigg(\int_0^b\int_0^a(X_mY_nX_mY_n)\mathrm{d}x\,\mathrm{d}y-\mu\Bigg(\int_0^b\int_0^a\left(\frac{\partial^2X_m}{\partial x^2}Y_nX_mY_n\right)\mathrm{d}x\,\mathrm{d}y$$
$$+\int_0^b\int_0^a\left(X_m\frac{\partial^2Y_n}{\partial y^2}X_mY_n\right)\mathrm{d}x\,\mathrm{d}y\Bigg)\Bigg)-(N^T+N^H+N^0-K_p)\Bigg(\int_0^b\int_0^a\left(\frac{\partial^2X_m}{\partial x^2}Y_nX_mY_n\right)\mathrm{d}x\,\mathrm{d}y$$
$$+\int_0^b\int_0^a\left(X_m\frac{\partial^2Y_n}{\partial y^2}X_mY_n\right)\mathrm{d}x\,\mathrm{d}y-\mu\Bigg(\int_0^b\int_0^a\left(\frac{\partial^4X_m}{\partial x^4}Y_nX_mY_n\right)\mathrm{d}x\,\mathrm{d}y$$
$$+2\int_0^b\int_0^a\left(\frac{\partial^2X_m}{\partial x^2}\frac{\partial^2Y_n}{\partial y^2}X_mY_n\right)\mathrm{d}x\,\mathrm{d}y+\int_0^b\int_0^a\left(X_m\frac{\partial^4Y_n}{\partial y^4}X_mY_n\right)\mathrm{d}x\,\mathrm{d}y\Bigg)\Bigg),\quad(50)$$

$$m_{1,1} = +I_0\left(\int_0^b\int_0^a\left(\frac{\partial X_m}{\partial x}Y_n\frac{\partial X_m}{\partial x}Y_n\right)\mathrm{d}x\,\mathrm{d}y - \mu\left(\int_0^b\int_0^a\left(\frac{\partial^3 X_m}{\partial x^3}Y_n\frac{\partial X_m}{\partial x}Y_n\right)\mathrm{d}x\,\mathrm{d}y + \int_0^b\int_0^a\left(\frac{\partial X_m}{\partial x}\frac{\partial^2 Y_n}{\partial y^2}\frac{\partial X_m}{\partial x}Y_n\right)\mathrm{d}x\,\mathrm{d}y\right)\right), \tag{51}$$

$$m_{1,2} = +I_0\left(\int_0^b\int_0^a\left(X_m\frac{\partial Y_n}{\partial y}X_m\frac{\partial Y_n}{\partial y}\right)\mathrm{d}x\,\mathrm{d}y - \mu\left(\int_0^b\int_0^a\left(X_m\frac{\partial^3 Y_n}{\partial y^3}X_m\frac{\partial Y_n}{\partial y}\right)\mathrm{d}x\,\mathrm{d}y + \int_0^b\int_0^a\left(\frac{\partial^2 X_m}{\partial x^2}\frac{\partial Y_n}{\partial y}X_m\frac{\partial Y_n}{\partial y}\right)\mathrm{d}x\mathrm{d}y\right)\right), \tag{52}$$

$$m_{3,1} = -I_1\left(\int_0^b\int_0^a\left(\frac{\partial X_m}{\partial x}Y_n\frac{\partial X_m}{\partial x}Y_n\right)\mathrm{d}x\,\mathrm{d}y - \mu\left(\int_0^b\int_0^a\left(\frac{\partial^3 X_m}{\partial x^3}Y_n\frac{\partial X_m}{\partial x}Y_n\right)\mathrm{d}x\,\mathrm{d}y + \int_0^b\int_0^a\left(\frac{\partial X_m}{\partial x}\frac{\partial^2 Y_n}{\partial y^2}\frac{\partial X_m}{\partial x}Y_n\right)\mathrm{d}x\,\mathrm{d}y\right)\right), \tag{53}$$

$$m_{4,1} = -I_3\left(\int_0^b\int_0^a\left(\frac{\partial X_m}{\partial x}Y_n\frac{\partial X_m}{\partial x}Y_n\right)\mathrm{d}x\,\mathrm{d}y - \mu\left(\int_0^b\int_0^a\left(\frac{\partial^3 X_m}{\partial x^3}Y_n\frac{\partial X_m}{\partial x}Y_n\right)\mathrm{d}x\,\mathrm{d}y + \int_0^b\int_0^a\left(\frac{\partial X_m}{\partial x}\frac{\partial^2 Y_n}{\partial y^2}\frac{\partial X_m}{\partial x}Y_n\right)\mathrm{d}x\,\mathrm{d}y\right)\right), \tag{54}$$

$$m_{3,2} = -I_1\left(\int_0^b\int_0^a\left(X_m\frac{\partial Y_n}{\partial y}X_m\frac{\partial Y_n}{\partial y}\right)\mathrm{d}x\,\mathrm{d}y - \mu\left(\int_0^b\int_0^a\left(X_m\frac{\partial^3 Y_n}{\partial y^3}X_m\frac{\partial Y_n}{\partial y}\right)\mathrm{d}x\,\mathrm{d}y + \int_0^b\int_0^a\left(\frac{\partial^2 X_m}{\partial x^2}\frac{\partial Y_n}{\partial y}X_m\frac{\partial Y_n}{\partial y}\right)\mathrm{d}x\,\mathrm{d}y\right)\right), \tag{55}$$

$$m_{4,2} = -I_3\left(\int_0^b\int_0^a\left(X_m\frac{\partial Y_n}{\partial y}X_m\frac{\partial Y_n}{\partial y}\right)\mathrm{d}x\,\mathrm{d}y - \mu\left(\int_0^b\int_0^a\left(X_m\frac{\partial^3 Y_n}{\partial y^3}X_m\frac{\partial Y_n}{\partial y}\right)\mathrm{d}x\,\mathrm{d}y + \int_0^b\int_0^a\left(\frac{\partial^2 X_m}{\partial x^2}\frac{\partial Y_n}{\partial y}X_m\frac{\partial Y_n}{\partial y}\right)\mathrm{d}x\,\mathrm{d}y\right)\right), \tag{56}$$

$$m_{3,3} = +I_0\left(\int_0^b\int_0^a(X_mY_nX_mY_n)\mathrm{d}x\,\mathrm{d}y - \mu\left(\int_0^b\int_0^a\left(\frac{\partial^2 X_m}{\partial x^2}Y_nX_mY_n\right)\mathrm{d}x\,\mathrm{d}y + \int_0^b\int_0^a\left(X_m\frac{\partial^2 Y_n}{\partial y^2}X_mY_n\right)\mathrm{d}x\,\mathrm{d}y\right)\right)$$
$$-I_2\left(\int_0^b\int_0^a\left(\frac{\partial^2 X_m}{\partial x^2}Y_nX_mY_n\right)\mathrm{d}x\,\mathrm{d}y + \int_0^b\int_0^a\left(X_m\frac{\partial^2 Y_n}{\partial y^2}X_mY_n\right)\mathrm{d}x\,\mathrm{d}y - \mu\left(\int_0^b\int_0^a\left(\frac{\partial^4 X_m}{\partial x^4}Y_nX_mY_n\right)\mathrm{d}x\,\mathrm{d}y\right.\right.$$
$$\left.\left. + 2\int_0^b\int_0^a\left(\frac{\partial^2 X_m}{\partial x^2}\frac{\partial^2 Y_n}{\partial y^2}X_mY_n\right)\mathrm{d}x\,\mathrm{d}y + \int_0^b\int_0^a\left(X_m\frac{\partial^4 Y_n}{\partial y^4}X_mY_n\right)\mathrm{d}x\,\mathrm{d}y\right)\right), \tag{57}$$

$$m_{3,4} = m_{4,3} = +I_0\left(\int_0^b\int_0^a(X_mY_nX_mY_n)\mathrm{d}x\,\mathrm{d}y - \mu\left(\int_0^b\int_0^a\left(\frac{\partial^2 X_m}{\partial x^2}Y_nX_mY_n\right)\mathrm{d}x\,\mathrm{d}y + \int_0^b\int_0^a\left(X_m\frac{\partial^2 Y_n}{\partial y^2}X_mY_n\right)\mathrm{d}x\,\mathrm{d}y\right)\right)$$
$$-I_4\left(\int_0^b\int_0^a\left(\frac{\partial^2 X_m}{\partial x^2}Y_nX_mY_n\right)\mathrm{d}x\,\mathrm{d}y + \int_0^b\int_0^a\left(X_m\frac{\partial^2 Y_n}{\partial y^2}X_mY_n\right)\mathrm{d}x\,\mathrm{d}y - \mu\left(\int_0^b\int_0^a\left(\frac{\partial^4 X_m}{\partial x^4}Y_nX_mY_n\right)\mathrm{d}x\,\mathrm{d}y\right.\right.$$
$$\left.\left. + 2\int_0^b\int_0^a\left(\frac{\partial^2 X_m}{\partial x^2}\frac{\partial^2 Y_n}{\partial y^2}X_mY_n\right)\mathrm{d}x\,\mathrm{d}y + \int_0^b\int_0^a\left(X_m\frac{\partial^4 Y_n}{\partial y^4}X_mY_n\right)\mathrm{d}x\,\mathrm{d}y\right)\right), \tag{58}$$

Table 1. Comparison of nondimensional fundamental natural frequency of FG nanoplates with simply-supported boundary conditions ($p = 5$).

a/h	μ	$a/b = 1$		$a/b = 2$	
		Natarajan *et al.* (2012)	present	Natarajan *et al.* (2012)	present
10	0	0.0441	0.043823	0.1055	0.104329
	1	0.0403	0.04007	0.0863	0.085493
	2	0.0374	0.037141	0.0748	0.074174
	4	0.0330	0.032806	0.0612	0.060673
20	0	0.0113	0.011256	0.0279	0.027756
	1	0.0103	0.010288	0.0229	0.022722
	2	0.0096	0.009534	0.0198	0.019704
	4	0.0085	0.008418	0.0162	0.016110

$$m_{4,4} = +I_0\left(\int_0^b\int_0^a (X_m Y_n X_m Y_n)\mathrm{d}x\,\mathrm{d}y - \mu\left(\int_0^b\int_0^a\left(\frac{\partial^2 X_m}{\partial x^2}Y_n X_m Y_n\right)\mathrm{d}x\,\mathrm{d}y + \int_0^b\int_0^a\left(X_m\frac{\partial^2 Y_n}{\partial y^2}X_m Y_n\right)\mathrm{d}x\,\mathrm{d}y\right)\right)$$

$$-I_5\left(\int_0^b\int_0^a\left(\frac{\partial^2 X_m}{\partial x^2}Y_n X_m Y_n\right)\mathrm{d}x\,\mathrm{d}y + \int_0^b\int_0^a\left(X_m\frac{\partial^2 Y_n}{\partial y^2}X_m Y_n\right)\mathrm{d}x\,\mathrm{d}y - \mu\left(\int_0^b\int_0^a\left(\frac{\partial^4 X_m}{\partial x^4}Y_n X_m Y_n\right)\mathrm{d}x\,\mathrm{d}y\right.\right.$$

$$\left.\left. + 2\int_0^b\int_0^a\left(\frac{\partial^2 X_m}{\partial x^2}\frac{\partial^2 Y_n}{\partial y^2}X_m Y_n\right)\mathrm{d}x\,\mathrm{d}y + \int_0^b\int_0^a\left(X_m\frac{\partial^4 Y_n}{\partial y^4}X_m Y_n\right)\mathrm{d}x\,\mathrm{d}y\right)\right). \tag{59}$$

Also, nondimensional parameters are defined as

$$K_w = \frac{k_w a^4}{D_c}, \qquad K_p = \frac{k_p a^2}{D_c}, \qquad D_c = \frac{E_c h^3}{12(1-v_c^2)}, \qquad \mu = \frac{ea}{a}, \qquad \lambda = \frac{l}{a}. \tag{60}$$

Finally, setting the coefficient matrix to zero gives the natural frequencies. The function X_m for simply-supported boundary conditions is defined by

$$X_m(x) = \sin(\lambda_m x)$$
$$\lambda_m = \frac{m\pi}{a}. \tag{61}$$

The function Y_n can be obtained by replacing x, m and a, respectively, by y, n and b.

5 Numerical results and discussions

Dynamic characteristics of size-dependent porous FG nanoplates are examined based on nonlocal strain gradient theory. The nanoplate is subjected to an in-plane periodic mechanical load. Hamilton's principle is employed to derive the governing equations. These equations have been expressed in the context of Mathieu-Hill equations and Bolotin's approach is implemented to evaluate the instability boundaries. Exactness of obtained vibration frequencies via four-variable plate model are verified with those of first-order shear deformation theory obtained by Natarajan *et al.* [36] using finite element method and the results are tabulated in table 1. It is noticeable that the presented Galerkin solution as well as the higher-order plate model can accurately predict the vibrational behavior of FG nanoplates.

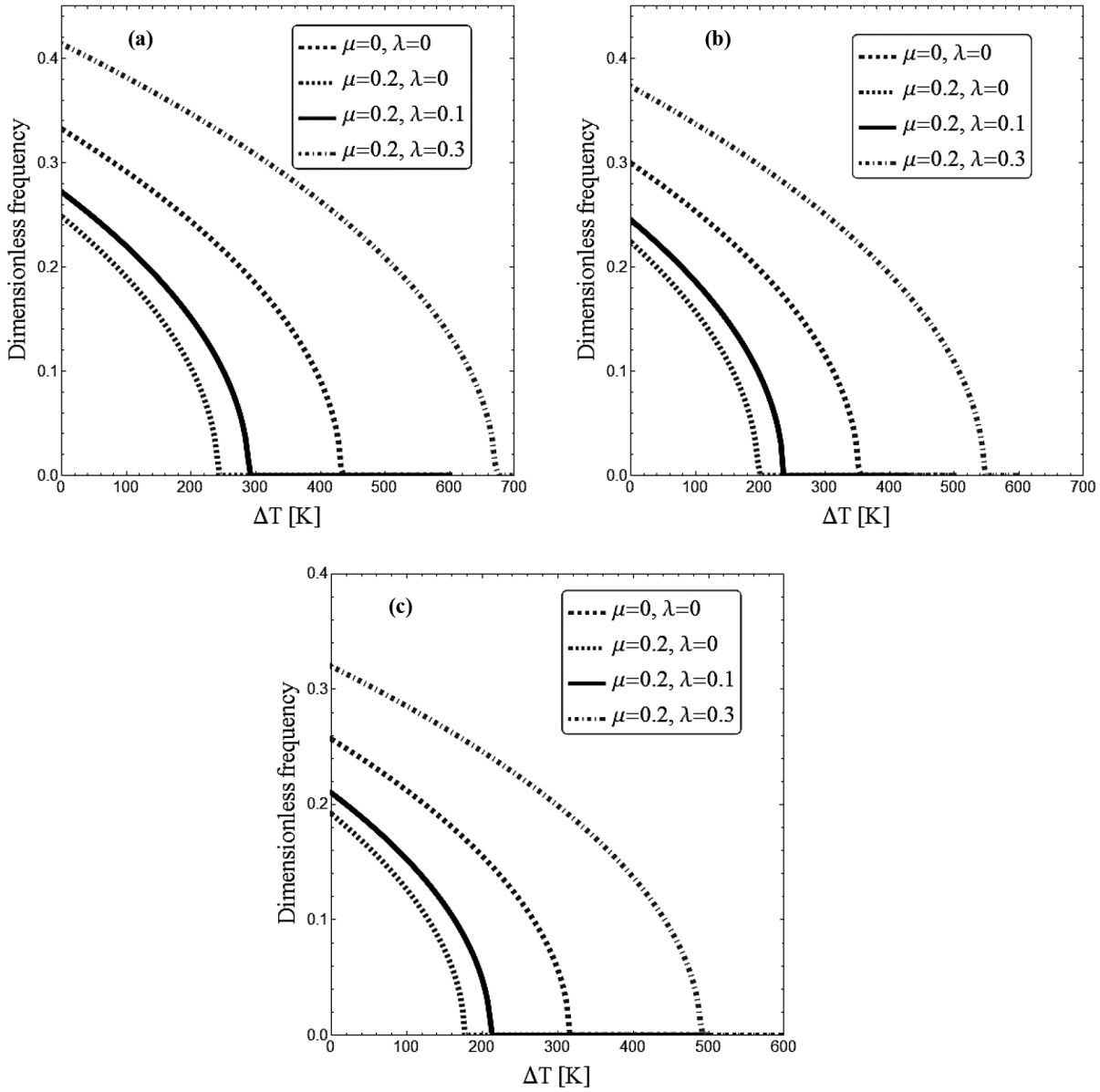

Fig. 2. Variation of dimensionless frequency of perfect nanoplate *versus* temperature rise for different nonlocal and strain gradient parameters ($a/h = 20$, $K_w = 0$, $K_p = 0$, $\Delta C = 0\%$).

The length of the nanoplate is assumed to be as $a = 10\,\text{nm}$. Also, the material properties of the nanoplate (alumina and aluminum) are considered as follows:

- $E_c = 380\,\text{GPa}$, $\rho_c = 3800\,\text{kg/m}^3$, $v_c = 0.3$, $\alpha_c = 7 \times 10^{-6}\,1/°\text{C}$, $\beta_c = 0.001$ (wt.% H_2o)$^{-1}$,
- $E_m = 70\,\text{GPa}$, $\rho_m = 2707\,\text{kg/m}^3$, $v_m = 0.3$, $\alpha_m = 23 \times 10^{-6}\,1/°\text{C}$, $\beta_m = 0.44$ (wt.% H_2o)$^{-1}$.

Investigation of the effects of moisture percentage rise and inhomogeneity index on the variation of free vibration frequencies of porous FG nanoplates is performed in fig. 3 for different elastic foundation parameters. The moisture percentage rise leads to lower bending rigidity of nanoplates and lower frequencies. Another interesting observation is that there is a large gap increasing the inhomogeneity index. In fact, with the increase in the inhomogeneity index (p), the influence of hygro-thermal loading increases. This is due to the excellent characteristics of ceramic to block the moisture. Therefore, increasing the metal portion with increasing the inhomogeneity index reveals that the humidity effect is increased in the structures. Consequently, FG materials are distinct from the conventional composite materials in the hygro-thermal mechanism, and the structure is more affected by the moisture at larger power-law indices. However, the elastic medium has an increasing effect on natural frequencies of FG nanoplates. In fact, increase in the Winkler and Pasternak constants yields enhancement of bending rigidity of the FG nanoplate.

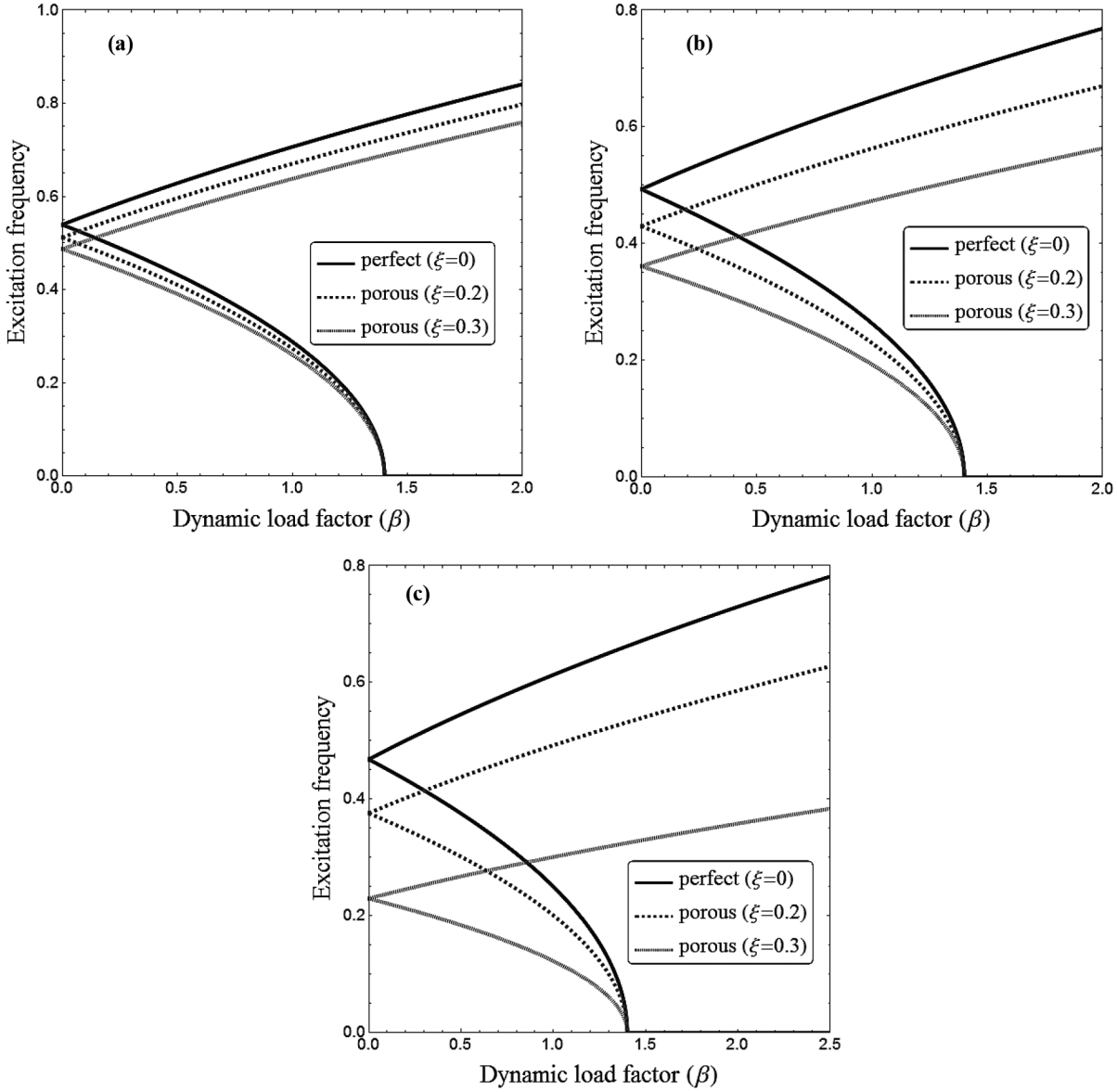

Fig. 3. Dimensionless frequency of the nanoplate *versus* dynamic load factor for different gradient index and porosity volume fractions ($a/h = 10$, $\alpha = 0.3$, $K_w = 0$, $K_p = 0$).

Free vibration frequency of a FG nanoplate with respect to the temperature rise is plotted in fig. 2 for different nonlocal (μ) and stain gradient (λ) parameters. It is observed that an increase in the temperature yields a reduction in both rigidity and natural frequencies of the FG nanoplate. At a certain temperature, the natural frequency of the nanoplate becomes zero. At this critical temperature, the nanoplate is buckled and does not oscillate. It is found that natural frequencies and critical buckling temperatures of FG nanoplates are significantly influenced by the value of nonlocal and strain gradient parameters. In fact, the nonlocal parameter introduces a stiffness-softening mechanism, while the strain gradient parameter provides a stiffness-hardening mechanism. In other words, increasing the nonlocal parameter leads to smaller frequencies and critical temperatures. In contrast, increasing the strain gradient parameter yields larger frequencies and critical temperatures. When λ is smaller than μ, obtained frequency is smaller than that of nonlocal elasticity theory. However, when λ is bigger than μ obtained frequencies becomes larger than nonlocal elasticity theory.

The porosity effect on the stability boundaries of FG nanoplates with respect to the dynamic load factor is presented in fig. 3 at $\mu = 0.2$, $\alpha = 0.3$, $K_w = 0$ and $K_p = 0$ for different material inhomogeneity index (p). Porosities inside the material lead to smaller frequencies by reducing the stiffness of the nanoplate. However, the instability region becomes smaller with the increase of porosity volume fraction. Therefore, a porous FG nanoplate under periodic in-plane loads is more stable than a perfect one. It can be also deduced that by reducing the gradient index, the width of the

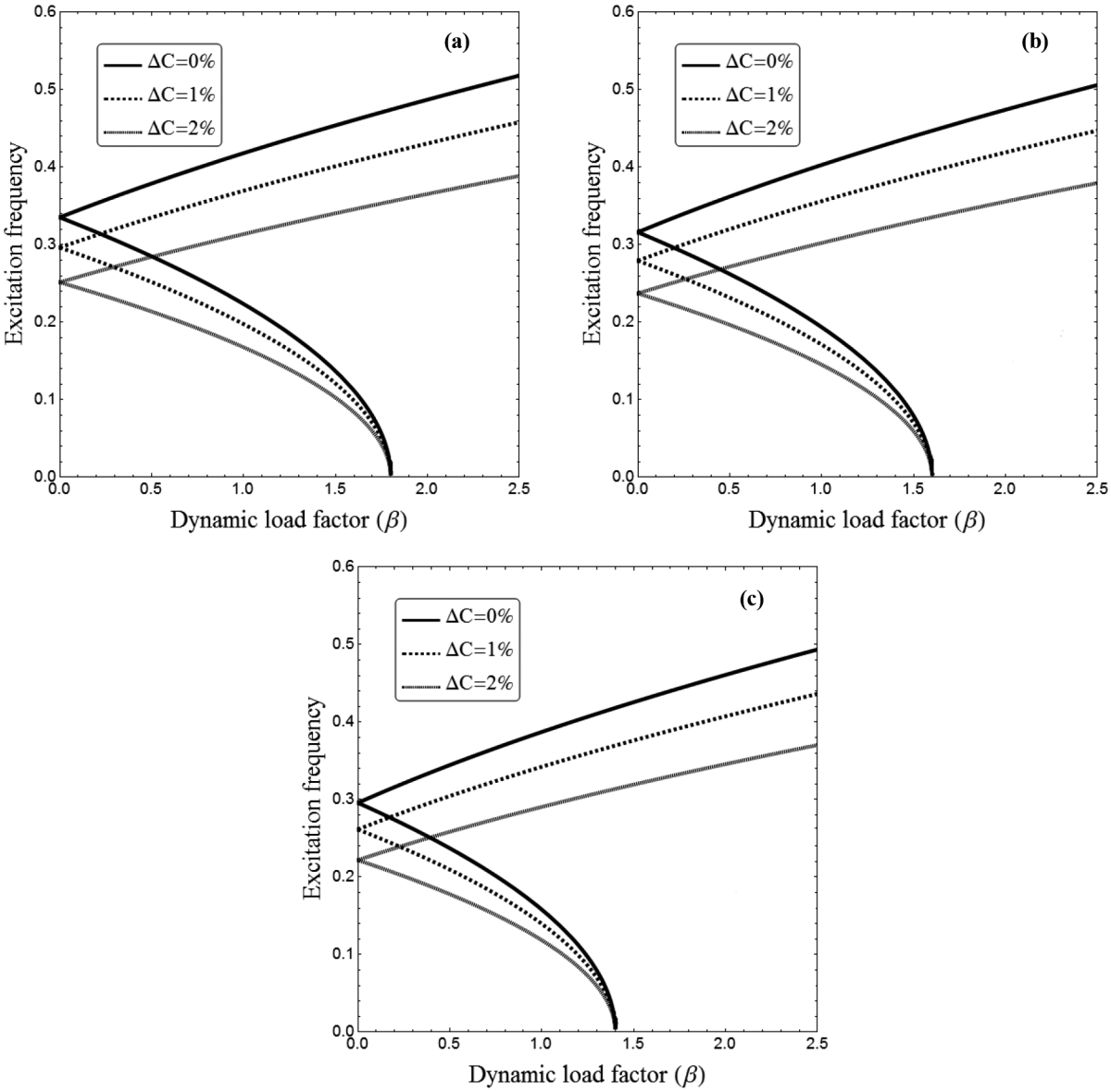

Fig. 4. Dimensionless frequency of the nanoplate *versus* dynamic load factor for different moisture percentage rises and static load factors ($a/h = 10$, $p = 1$, $\Delta T = 0$, $\xi = 0.1$, $K_w = 0$, $K_p = 0$, $\mu = 0.2$, $\lambda = 0.1$).

instability region increases. Also, it is observed that as the gradient index rises, the magnitude of the nondimensional excitation frequency increases at a fixed dynamic load factor. Therefore, material gradation plays a major role on the unstable region and should be considered in the dynamic analysis of nanoplates.

Figure 4 shows the influence of static load factor (α) and moisture percentage rise on the dynamic stability characteristics of size-dependent FGM nanoplates at $a/h = 10$, $p = 1$ and $K_w = K_p = 0$. It can be observed, in the figure, that when the moisture percentage increases, the dynamic buckling boundaries decrease. It means that the parametric instability can be enhanced by the moisture change. However, the starting point ($\beta = 0$) is reduced with the increase in the moisture percentage. The reason is that the existence of a humidity field diminishes the bending rigidity of the FG nanoplates leading to a reduction in the frequencies. According to this figure, when the static load factor rises, the boundaries of dynamic instability region reduce at a fixed nonlocal parameter. This is due to the fact that compressive static load reduces the flexibility of the FGM nanoplate, and leads to smaller excitation frequencies. One can see that the instability region of FGM nanoplates becomes closer to the origin by increasing the magnitude of static load factor.

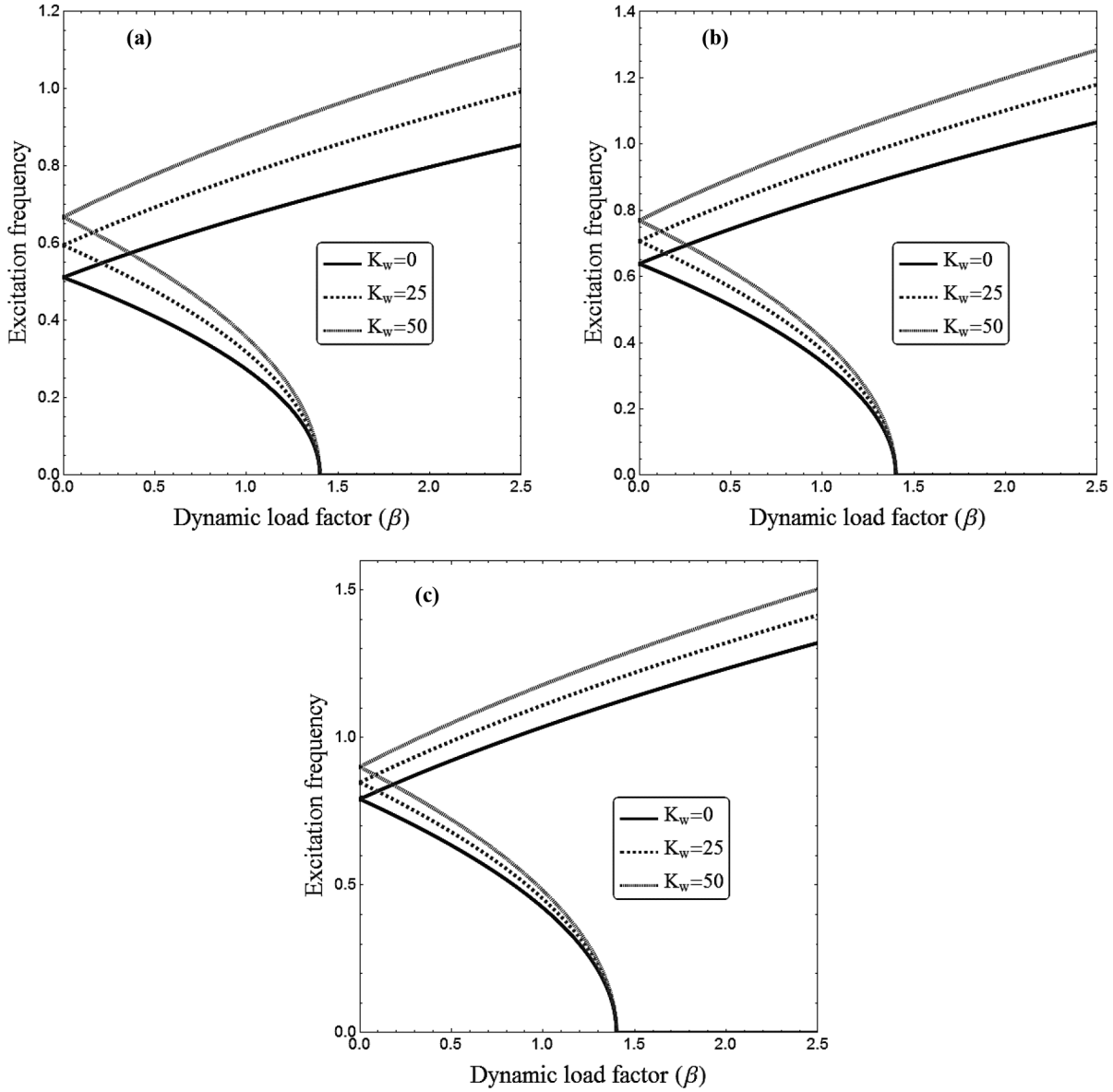

Fig. 5. Dimensionless frequency of the nanoplate *versus* dynamic load factor for various foundation constants ($a/h = 10$, $\alpha = 0.3$, $p = 1$, $\Delta T = 0$, $\mu = 0.2$, $\lambda = 0.01$).

In fig. 5, the variation of the dimensionless excitation frequency with respect to the dynamic load factor for various elastic foundation constants is studied for simply-supported nanoplates when $p = 1$, $\alpha = 0.3$ and $\mu = 0.2$. It is observable that increasing the foundation constants gives larger magnitudes of nondimensional excitation frequency. In fact, with increasing foundation constants, *i.e.* overall increase in the plate rigidity, the dynamic buckling boundaries are transferred to the upper points of origin. Although both Winkler and Pasternak constants yield larger excitation frequencies, one can see that the Pasternak's constant has more increasing influence on the dimensionless excitation frequency compared to the Winkler constant. Therefore, the shear layer of the elastic foundation, called Pasternak foundation, plays an important role on the instability behavior of FGM nanoplates.

Figure 6 shows the variation of nondimensional free vibration frequency of FG nanoplates *versus* the moisture percentage rise for various side-to-thickness ratios (a/h) at $\Delta T = 50$, $K_w = 25$, $K_p = 10$, $\xi = 0.05$, $\mu = 0.2$ and $\lambda = 0.1$. As previously mentioned, increasing the side-to-thickness ratio gives smaller natural frequencies. The reason is more flexibility of the nanoplate with an increase in the side-to-thickness ratio. Also, it is found that the FG nanoplates with higher side-to-thickness ratios are more affected by the moisture rise. In fact, natural frequency of a FG nanoplate at high side-to-thickness ratios reduces with a higher rate with respect to moisture percentage rise than a nanoplate with a small side-to-thickness ratio.

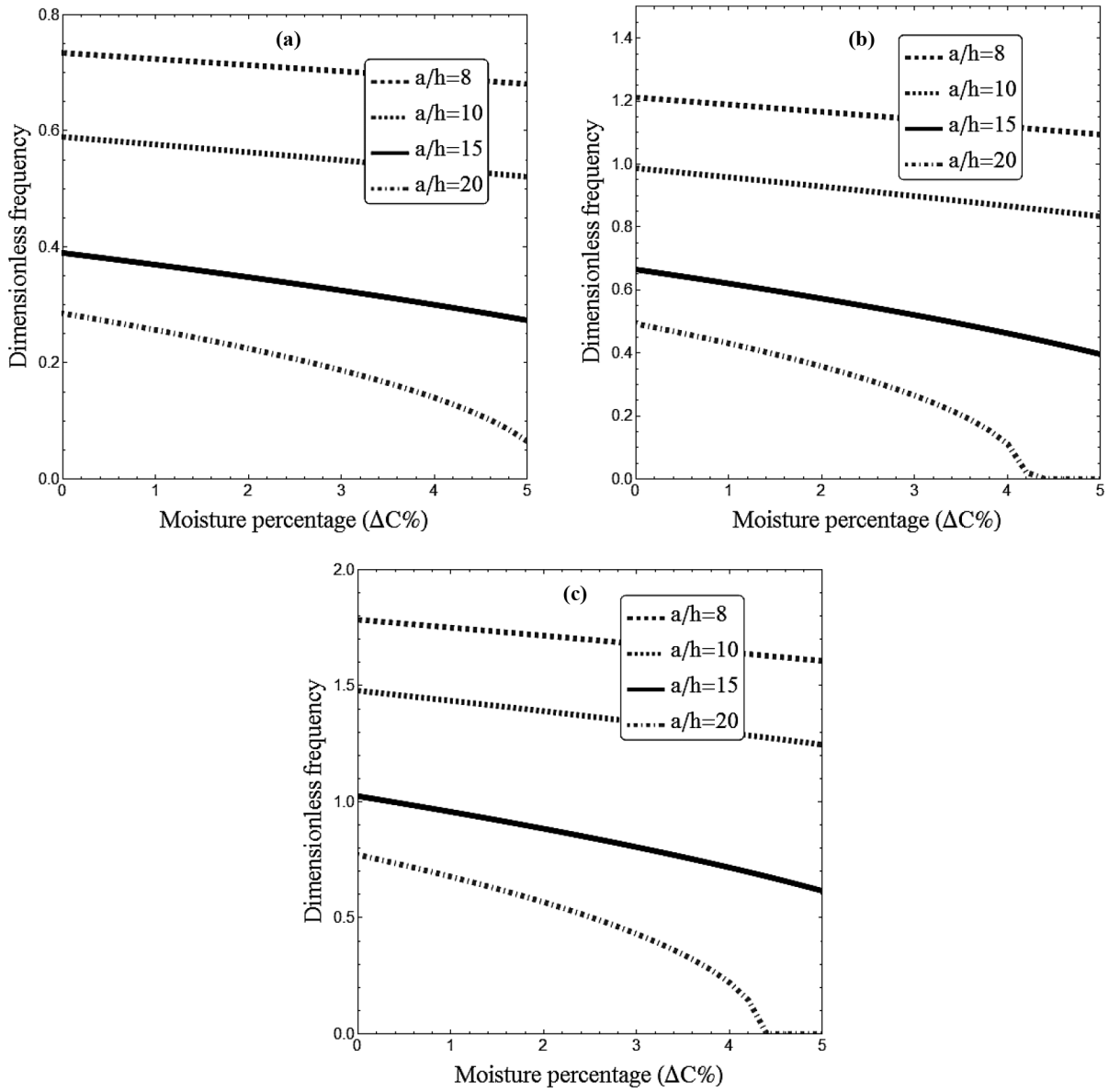

Fig. 6. Variation of dimensionless frequency of porous nanoplates *versus* moisture percentage for different aspect ratios ($\Delta T = 50$, $K_w = 25$, $K_p = 10$, $\mu = 0.2$, $\lambda = 0.1$).

6 Conclusions

Based on generalized nonlocal strain gradient theory, dynamic analysis of inhomogeneous nanoplates with porosities is presented for the first time. Therefore, it is possible to capture both stiffness-softening and stiffness-hardening effects for a more accurate vibration analysis of nanoplates. The nanoplate is in hygro-thermal environments and it is subjected to an in-plane harmonic load. Increase in the nonlocality leads to lower resonance frequencies, while increase in the strain gradient parameter leads to larger resonance frequencies. It is also shown that the proposed higher-order refined theory provides a more accurate estimation of the resonance frequency of a nanoplate. It is concluded that the instability region is wider for FGM nanoplates with larger magnitudes of the Winkler's and Pasternak's constants. The Pasternak's elastic foundation constant has a higher impact on increasing the instability regions than the Winkler's constant.

References

1. K. Kiani, Int. J. Eng. Sci. **106**, 57 (2016).
2. C.Y. Lee, J.H. Kim, Compos. Struct. **95**, 278 (2013).
3. M. Zidi, A. Tounsi, M.S.A. Houari, O.A. Bég, Aerospace Sci. Technol. **34**, 24 (2014).
4. B. Akgöz, Ö. Civalek, Int. J. Eng. Sci. **85**, 90 (2014).
5. M. Sobhy, Int. J. Mech. Sci. **110**, 62 (2016).
6. H. Matsunaga, Compos. Struct. **90**, 76 (2009).
7. S.S. Vel, R.C. Batra, Int. J. Solids Struct. **40**, 7181 (2003).
8. Y. Khalfi, M.S.A. Houari, A. Tounsi, Int. J. Comput. Methods **11**, 1350077 (2014).
9. Z. Lee, C. Ophus, L.M. Fischer, N. Nelson-Fitzpatrick, K.L. Westra, S. Evoy, V. Radmilovic, U. Dahmen, D. Mitlin, Nanotechnology **17**, 3063 (2006).
10. Yumin Ye, in *Biofunctional Polymer Coatings via Initiated Chemical Vapor Deposition* (Shareok, 2015) appendix A.
11. F. Mao, M. Taher, O. Kryshtal, A. Kruk, A. Czyrska-Filemonowicz, M. Ottosson, U. Jansson, ACS Appl. Mater. Interfaces **8**, 30635 (2016).
12. J. Zalesak, M. Bartosik, R. Daniel, C. Mitterer, C. Krywka, D. Kiener, J. Keckes, Acta Mater. **102**, 212 (2016).
13. C.F. Lü, W.Q. Chen, C.W. Lim, Compos. Sci. Technol. **69**, 1124 (2009).
14. H. Salehipour, A.R. Shahidi, H. Nahvi, Int. J. Eng. Sci. **90**, 44 (2015).
15. H.M. Sedighi, F. Daneshmand, M. Abadyan, Compos. Struct. **132**, 545 (2015).
16. A.C. Eringen, D.G.B. Edelen, Int. J. Eng. Sci. **10**, 233 (1972).
17. A.C. Eringen, J. Appl. Phys. **54**, 4703 (1983).
18. H.T. Thai, Int. J. Eng. Sci. **52**, 56 (2012).
19. F. Ebrahimi, M.R. Barati, Smart Mater. Struct. **26**, 065018 (2017).
20. F. Ebrahimi, M.R. Barati, Int. J. Eng. Sci. **107**, 183 (2016).
21. M.Z. Nejad, A. Hadi, Int. J. Eng. Sci. **105**, 1 (2016).
22. A.G. Arani, M.H. Jalaei, Int. J. Eng. Sci. **103**, 97 (2016).
23. C. Li, J.J. Liu, M. Cheng, X.L. Fan, Compos. Part B: Eng. **116**, 153 (2017).
24. A. Naderi, A.R. Saidi, Int. J. Eng. Sci. **81**, 49 (2014).
25. F. Ebrahimi, M.R. Barati, Eur. Phys. J. Plus **132**, 19 (2017).
26. F. Ebrahimi, M.R. Barati, Eur. Phys. J. Plus **131**, 279 (2016).
27. I.R. Pavlović, D. Karličić, R. Pavlović, G. Janevski, I. Ćirić, Int. J. Eng. Sci. **109**, 88 (2016).
28. Y. Lei, S. Adhikari, M.I. Friswell, Int. J. Eng. Sci. **66**, 1 (2013).
29. A. Khajeansari, G.H. Baradaran, J. Yvonnet, Int. J. Eng. Sci. **52**, 115 (2012).
30. M.Z. Nejad, A. Hadi, Int. J. Eng. Sci. **106**, 1 (2016).
31. J.C. Liu, Y.Q. Zhang, L.F. Fan, Phys. Lett. A **381**, 1228 (2017).
32. M.Z. Nejad, A. Hadi, A. Rastgoo, Int. J. Eng. Sci. **103**, 1 (2016).
33. C.P. Wu, W.C. Li, Comput. Math. Appl. **73**, 838 (2017).
34. H.T. Thai, T.P. Vo, Int. J. Eng. Sci. **54**, 58 (2012).
35. C.M.C. Roque, A.J.M. Ferreira, J.N. Reddy, Int. J. Eng. Sci. **49**, 976 (2011).
36. S. Natarajan, S. Chakraborty, M. Thangavel, S. Bordas, T. Rabczuk, Comput. Mater. Sci. **65**, 74 (2012).
37. A. Daneshmehr, A. Rajabpoor, Int. J. Eng. Sci. **82**, 84 (2014).
38. M.R. Nami, M. Janghorban, Compos. Struct. **111**, 349 (2014).
39. R. Ansari, M.F. Shojaei, A. Shahabodini, M. Bazdid-Vahdati, Compos. Struct. **131**, 753 (2015).
40. A. Daneshmehr, A. Rajabpoor, A. Hadi, Int. J. Eng. Sci. **95**, 23 (2015).
41. I. Belkorissat, M.S.A. Houari, A. Tounsi, E.A. Bedia, S.R. Mahmoud, Steel Compos. Struct. **18**, 1063 (2015).
42. M.R. Barati, Appl. Phys. A **123**, 332 (2017).
43. F. Ebrahimi, M.R. Barati, Appl. Phys. A **122**, 910 (2016).
44. F. Ebrahimi, A. Dabbagh, M.R. Barati, Eur. Phys. J. Plus **131**, 433 (2016).
45. F. Ebrahimi, M.R. Barati, J. Braz. Soc. Mech. Sci. Eng. **39**, 2203 (2017).
46. M. Sobhy, Compos. Struct. **134**, 966 (2015).
47. K. Khorshidi, A. Fallah, Int. J. Mech. Sci. **113**, 94 (2016).
48. M. Sobhy, A.F. Radwan, Int. J. Appl. Mech. **9**, 1750008 (2017).
49. D.C. Lam, F. Yang, A.C.M. Chong, J. Wang, P. Tong, J. Mech. Phys. Solids **51**, 1477 (2003).
50. C.W. Lim, G. Zhang, J.N. Reddy, J. Mech. Phys. Solids **78**, 298 (2015).
51. L. Li, Y. Hu, L. Ling, Compos. Struct. **133**, 1079 (2015).
52. L. Li, X. Li, Y. Hu, Int. J. Eng. Sci. **102**, 77 (2016).
53. M. Şimşek, Int. J. Eng. Sci. **105**, 12 (2016).
54. L. Li, Y. Hu, Int. J. Mech. Sci. **120**, 159 (2017).
55. F. Ebrahimi, M.R. Barati, Compos. Struct. **159**, 433 (2017).
56. F. Ebrahimi, M.R. Barati, Proc. Inst. Mech. Eng. C (2016) https://doi.org/10.1177/0954406216668912.
57. A. Farajpour, M.H. Yazdi, A. Rastgoo, M. Mohammadi, Acta Mech. **227**, 1849 (2016).
58. M.R. Farajpour, A. Rastgoo, A. Farajpour, M. Mohammadi, Micro Nano Lett. **11**, 302 (2016).
59. F. Ebrahimi, M.R. Barati, A. Dabbagh, Int. J. Eng. Sci. **107**, 169 (2016).
60. E.O. Alzahrani, A.M. Zenkour, M. Sobhy, Compos. Struct. **105**, 163 (2013).
61. M. Sobhy, Compos. Part B: Eng. **79**, 224 (2015).